**Description of Supplementary Files**

File Name: Supplementary Information
Description: Supplementary Figures and Supplementary Tables.

File Name: Supplementary Movie 1
Description: **Lymphatic organization in the mLN of naive mice** mLN LECs were imaged using light sheet microscopy and processed using IMARIS. The movie represents the temporal color code profile for LYVE-1 staining indicating the depth of LECs from the edge. LECs close to subcapsular sinus (SCS) appear more red where as LECs in paracortical region appears more blue. Movie 1 represents a naïve mLN where LECs are absent in the paracortical region (PCR). The blue region represents the medullary region.

File Name: Supplementary Movie 2
Description: **Lymphatic organization in the mLN of helminth infected mice** The movie represents the temporal color code profile for LYVE-1 staining indicating the depth of LECs from the edge. LECs close to subcapsular sinus (SCS) appear more red where as LECs in paracortical region appears more blue. Movie 2 represents 21dpi mLN.

File Name: Supplementary Movie 3
Description: **LECs penetrate deep into the paracortical region of the mLN** mLN LECs were imaged using light sheet microscope after 21dpi. 200 µm thick vibratome section (obtained from central part of mLN) was subjected to optical clearing before imaging. Z-stacks were acquired and processed using IMARIS. The movie shown represents the LYVE-1 staining from periphery to deep paracortical zone.

File Name: Supplementary Movie 4
Description: **Lymphatic network form a 'cup' like structure around B cell follicles post infection** 3D view of a vibratome section showing combined immunofluorescence staining for B cell follicles (B220; green) and LECs (LYVE-1; red) from mLN of 21dpi mice.

File Name: Supplementary Movie 5
Description: **Lymphatics form a 'cup' like structure around B cell follicles** 3D view of a vibratome section showing combined immunofluorescence staining for B cell follicles (B220; green) and LECs (LYVE-1; red) from mLN of naive mice.

File Name: Supplementary Movie 6
Description: **LECs and FRCs lie in close proximity to each other** Vibratome sections of paracortical regions inside 21 dpi mLN stained with the Lyve-1 (red), Podoplanin (grey) and DAPI (blue). Note the close proximity of paracortical lymphatic endothelial cells (as defined by LYVE-1+ ; red staining) and fibroblastic reticular cells (grey; PDPN+ LYVE-1- ).

File Name: Peer Review File

Supplementary Figure-1

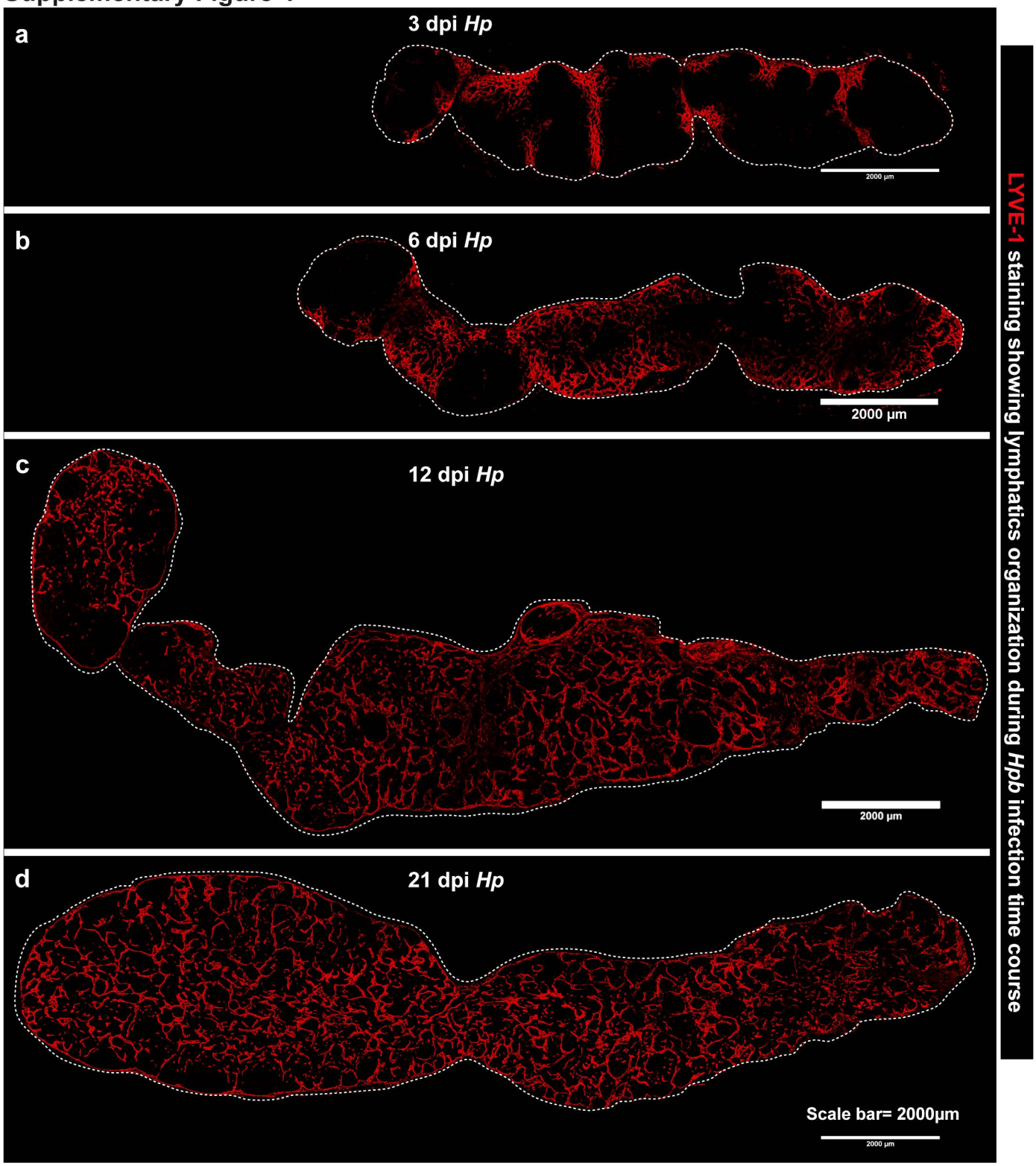



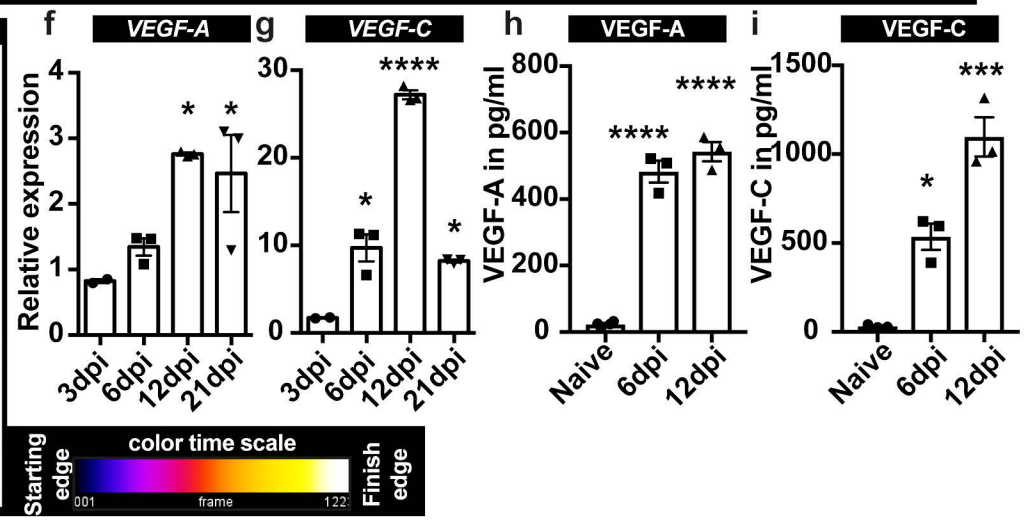

**Supplementary Figure-1**

**A timecourse of mLN lymphangiogenesis in the draining mLN following *Hp* infection**

C57BL/6J mice were infected with *Hp* and the entire chain of the mLN collected at the indicated time-points. **(a-d)** mLN serial cryosections showing lymphatics organization (red; $LYVE1^+$). Scale bar =2,000 μm. The dotted line outlines the outer capsule of the mLN. Images are representative of a single mouse from a total of five or more experiments. **(e)** LYVE-$1^+$ LECs network as visualized in a vibratome section of 21 dpi mLN by deep tissue imaging. Temporal color profile is used to indicate the lymphatic network in paracortical regions. **(f-g)** *Vegf-a* and *Vegf-c* mRNA expression during the infection time course as determined using real time PCR. **(h-i)** VEGF-A and C protein levels in mLN tissue lysate as determined by ELISA. Data represent mean ± SEM from a single experiment and are representative of two independent experiments each including n ≥2-3 mice per group/time point. Statistical analyses were performed using ANOVA, Bonferroni's multiple comparison test or Mann-Whitney test and significance donated as *$p < 0.05$, **$p < 0.01$, ***$p < 0.001$, and ****$p < 0.0001$

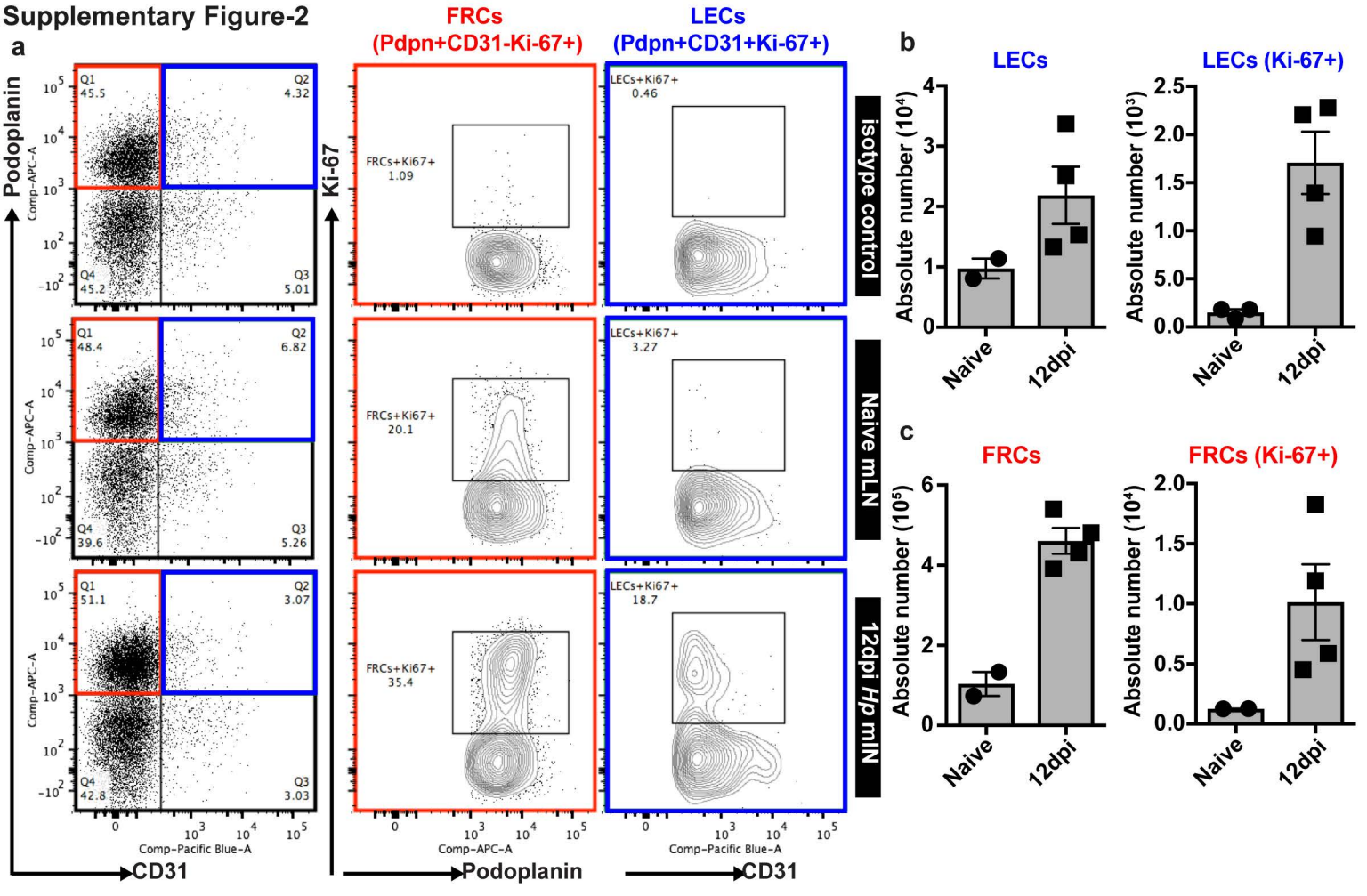
Supplementary Figure-2
a
FRCs
(Pdpn+CD31-Ki-67+)
LECs
(Pdpn+CD31+Ki-67+)
Podoplanin
Ki-67
CD31
Podoplanin
CD31
Comp-APC-A
Comp-Pacific Blue-A
Q1
45.5
Q2
4.32
Q4
45.2
Q3
5.01
FRCs+Ki67+
1.09
LECs+Ki67+
0.46
isotype control
Q1
48.4
Q2
6.82
Q4
39.6
Q3
5.26
FRCs+Ki67+
20.1
LECs+Ki67+
3.27
Naive mLN
Q1
51.1
Q2
3.07
Q4
42.8
Q3
3.03
FRCs+Ki67+
35.4
LECs+Ki67+
18.7
12dpi Hp mLN
b
LECs
LECs (Ki-67+)
Absolute number (10⁴)
Absolute number (10³)
Naive
12dpi
c
FRCs
FRCs (Ki-67+)
Absolute number (10⁵)
Absolute number (10⁴)
Naive
12dpi

**Supplementary Figure-2**

**Helminth infection elicits LECs and FRCs expansion and in the mLN**

Flow cytometric analysis of stromal proliferation phenotype. **(a)** Representative FACS contour plots showing Ki-67$^{+}$ FRCs (PDPN+CD31-) and LECs (PDPN+CD-31+) during naïve and after *Hpb* infection. **(b-c)** Histograms showing absolute number of proliferating FRCs and LECs post infection. Results are expressed as mean ± SEM.

# Supplementary Figure-3

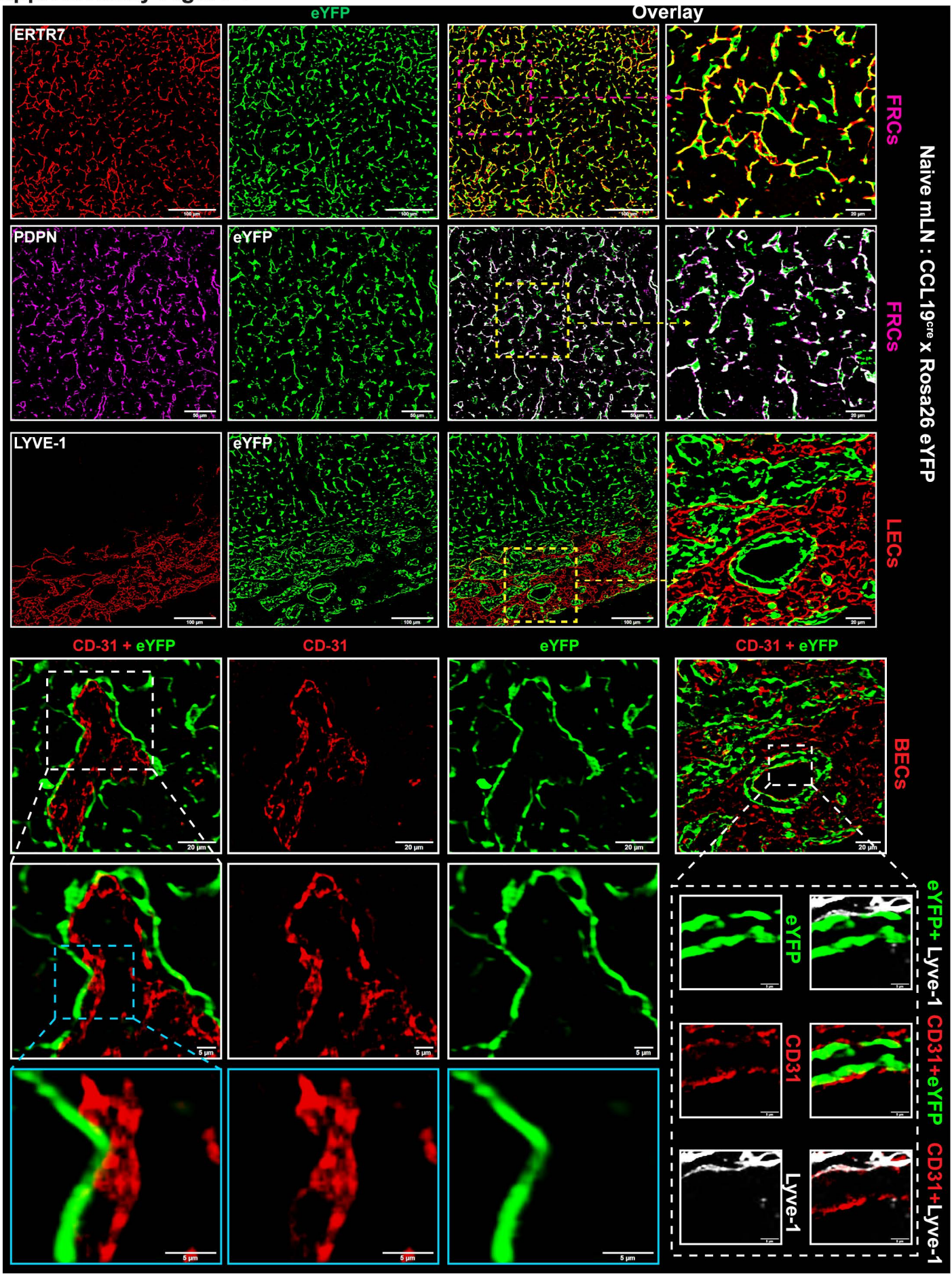

**Supplementary Figure-3**

***Ccl19*$^{Cre}$ expression is restricted to FRCs and not present in mLN LECs, BECs or in HEVs**

**(a-c)** mLN cryosections from a *Ccl19*$^{-cre}$ × *Rosa26*-eYFP reporter mouse showing combined immunofluorescence staining for eYFP (green, anti-GFP exhibiting cross-reactivity with eYFP) and stromal cells (red, ER-TR7; magenta, Podoplanin) or LECs (red, LYVE-1). **(d)** *Ccl19*$^{-cre}$ × *Rosa26-eYFP* reporter mouse showing combined immunofluorescence staining for eYFP alongside HEVs (Red, CD31$^{+}$) and BECs (Red, CD31$^{+}$) stromal cells. Scale bar = 100 and 20 μm.

Supplementary Figure-4

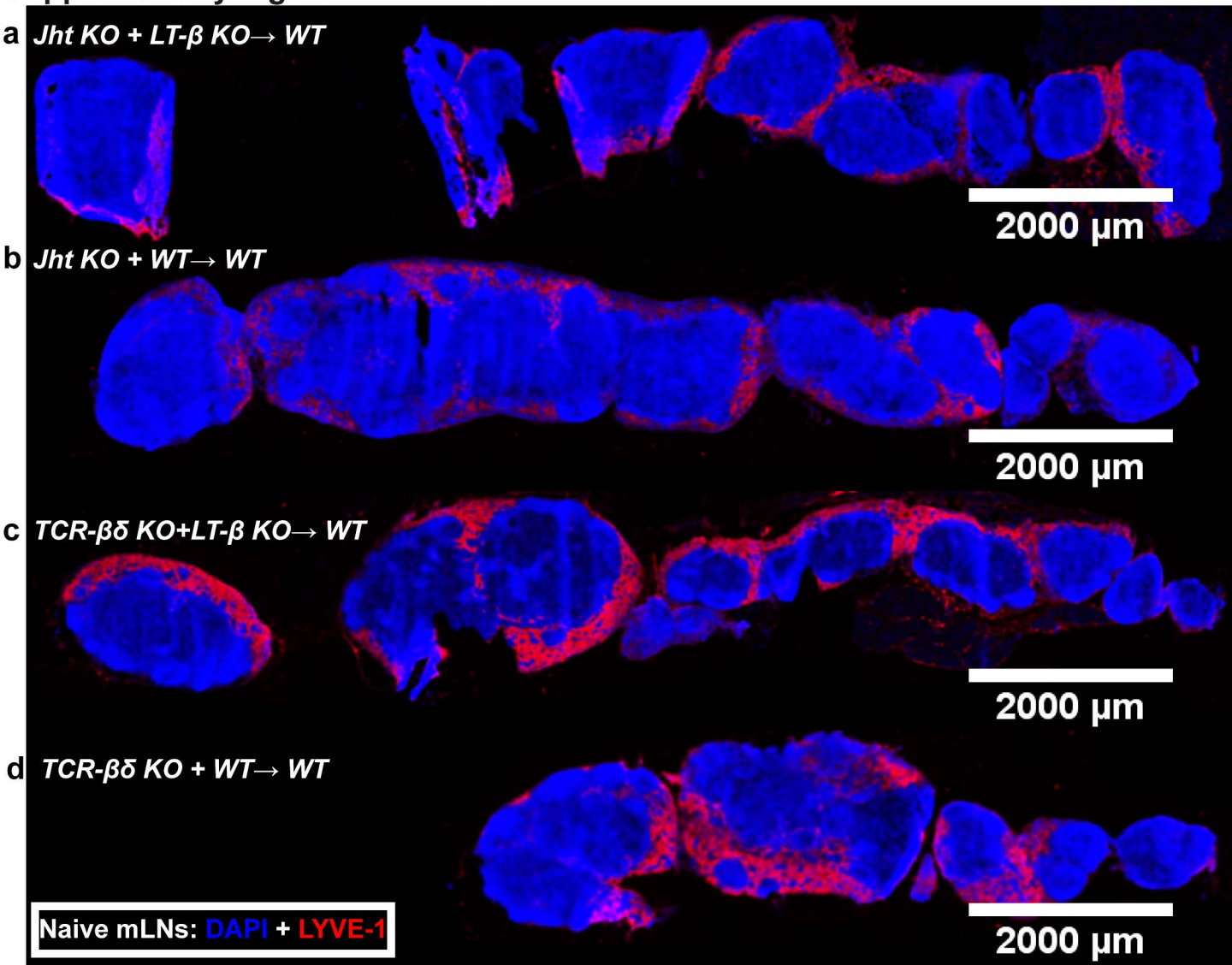

**Supplementary Figure-4**

**Lymphatic organization in the mLN of naive bone marrow chimera mice lacking lymphotoxin expression on B cells or T cells**

**(a-d)** Mixed bone marrow chimeras lacking lymphotoxin selectively on B cells (*Jht*$^{-/-}$ + *LTβ*$^{-/-}$) or T cells (*TCRβδ*$^{-/-}$ + *LTβ*$^{-/-}$) and control chimeras (*Jht*$^{-/-}$ + WT and *TCRβδ*$^{-/-}$ + WT) were generated and the mLN taken. Immunofluorescence images from naive mice mLN showing LECs network (LYVE-1$^{+}$; red). Scale bar =2000μm.

Supplementary Figure-5

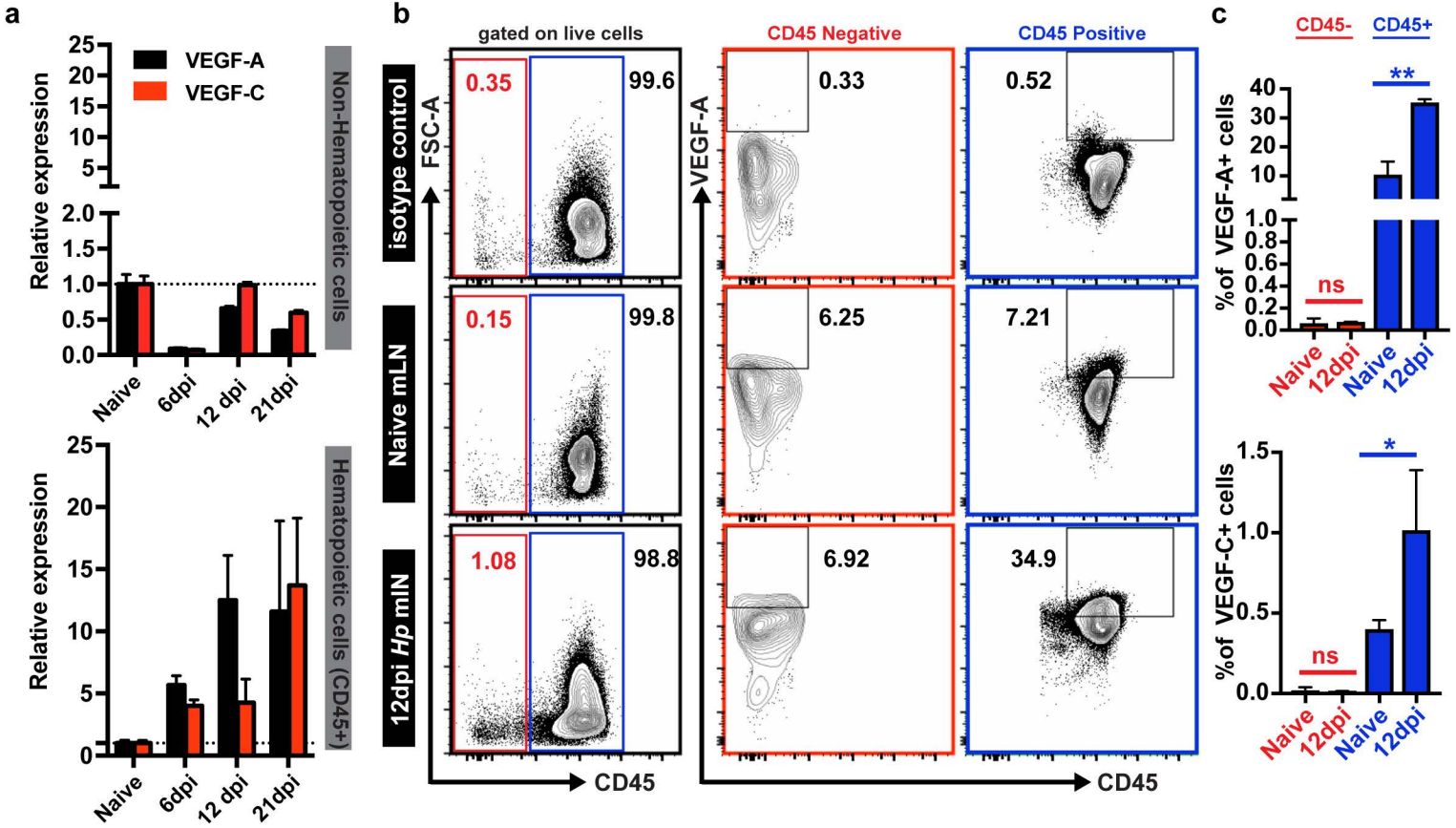

**Supplementary Figure-5**

**Hematopoietic cell type represents the dominant VEGF producing compartment in the mLN of *Hp* infected mice**

**(a)** Non-hematopoietic versus hematopoietic *VEGF-A* and *VEGF-C* mRNA expression during the infection time course as determined using real time PCR. Data represent mean ± SEM from a single experiment and are representative of two independent experiments each including n ≥2-3 mice per group/time point. **(b)** Gating strategy-showing identification of VEGFs producing hematopoietic and non-hematopoietic population. **(c)** Pooled data showing the percentage of VEGF-A/C$^{+}$ CD45$^{+}$ cells (blue histograms) and CD45$^{-}$ (red histograms) cells as determined in b.

Supplementary Figure-6

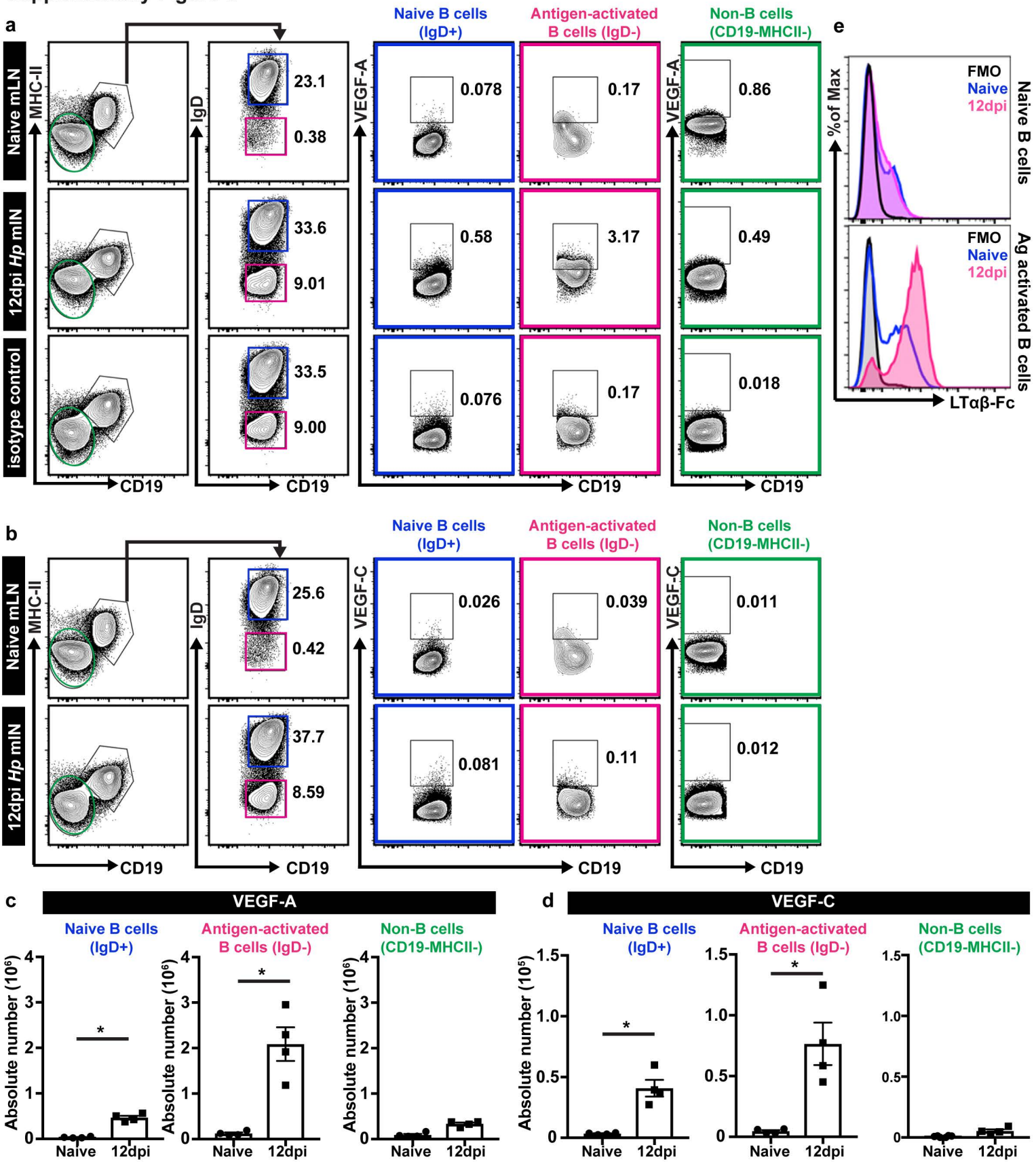

**Supplementary Figure-6**

**B cells represent the dominant VEGF producing hematopoietic cell type in the mLN of *Hp* infected mice**

**(a-b)** Representative dot plots showing gating strategy for identification of VEGFs producing naïve ($CD19^{+}MHC\text{-}II^{+}IgD^{+}$) and activated B cells ($CD19^{+}MHC\text{-}II^{+}IgD^{-}$) post infection. **(c-d)** Data showing the absolute number of $VEGFs^{+}$ naïve or activated B cells and non-B cells, as determined in **a-b**. **(e)** B cell lymphotoxin expression was determined by staining with LTβR-Fc. Histograms represent the lymphotoxin expression on naïve B cells (top panel) and activated B cells (bottom panel) during naïve and 12dpi mLN. Lymphotoxin expression was higher in activated B cells compared to naïve B cells at 12dpi (bottom panel). Data represent mean ± SEM from a single experiment and are representative of two or more independent experiments each including n=4 mice/group/time-point. Statistical analyses were performed using non parametric Mann-Whitney T test and significance donated as $*p < 0.05$.

Supplementary Figure-7

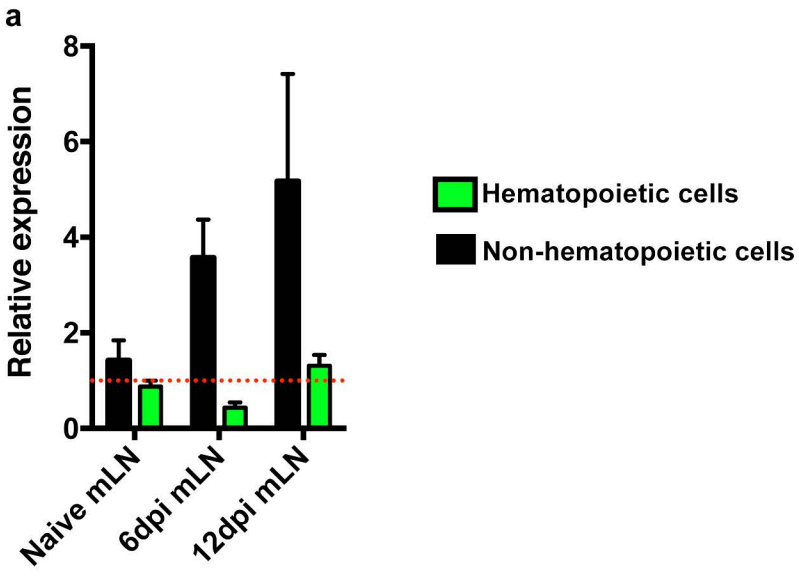


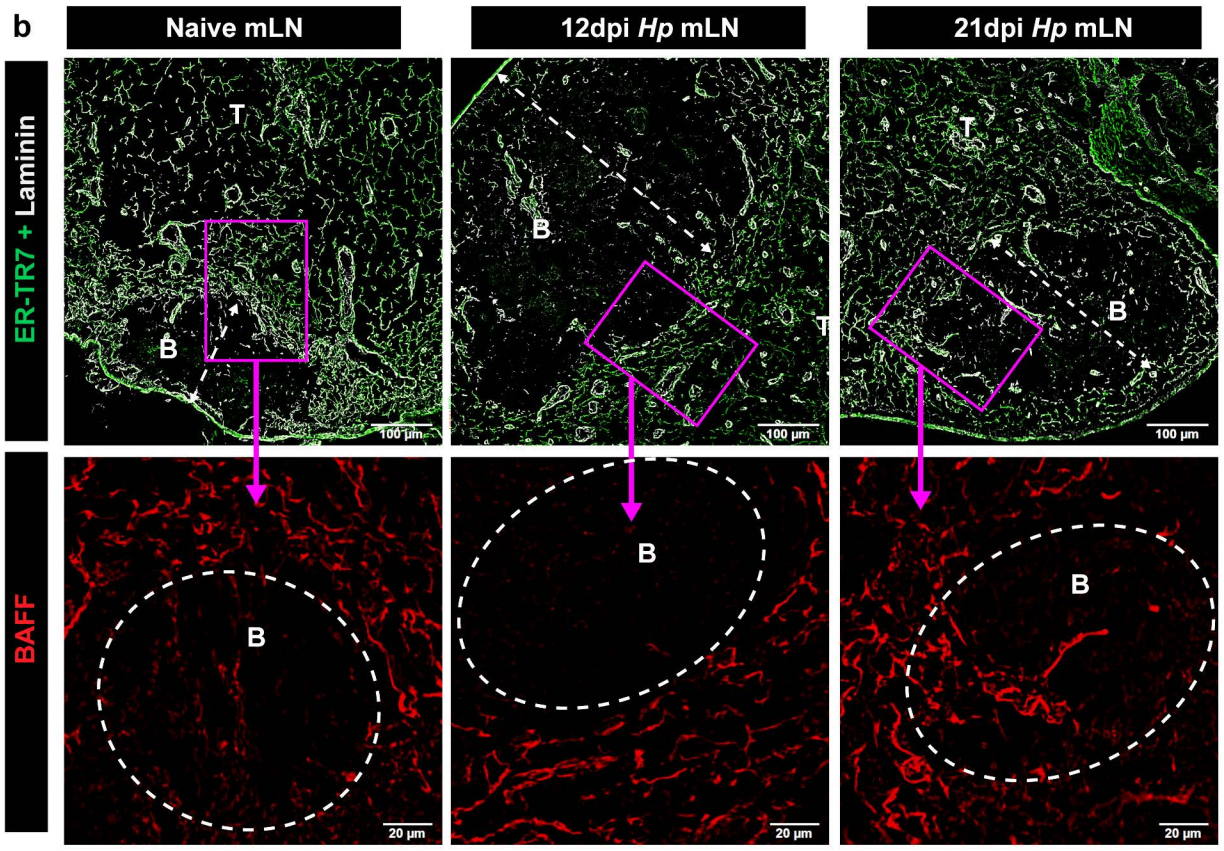

**Supplementary Figure-7**

**FRCs surround B cell follicles produce BAFF**

Wildtype C57BL/6 mice were infected with *Hp* and the entire chain of the mLN collected at the indicated time-points. **(a)** *BAFF* mRNA expression by mLN stromal (non-hematopoietic cells) versus cellular (hematopoietic cells) components following *Hp* infection. Data represent mean ± SEM, and are representative of two independent experiments with n ≥2-3 mice per group/time point. **(b)** Images of mLN cryosections showing BAFF protein (red) and FRCs (green, ER-TR7$^{+}$; white, laminin$^{+}$) around a B cell follicle. Scale bar = 100 μm. B cell follicles are outlined by a white dotted line and arrows indicate the change in follicle size post infection. Magenta insets are also shown at higher magnification (Scale bar = 20 μm) and show BAFF expression at the mantle region of B cell follicle.

Supplementary Figure-8

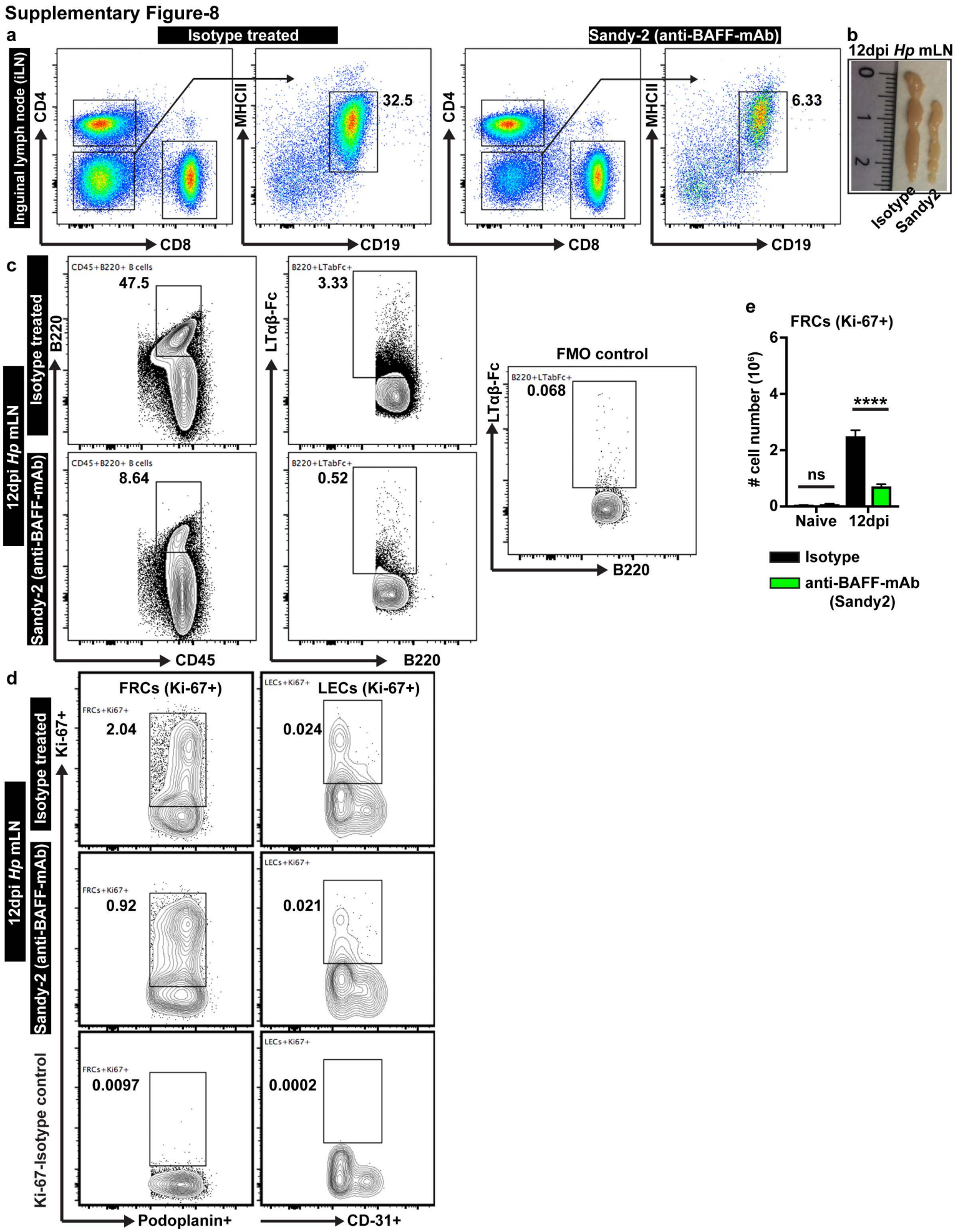

**Supplementary Figure-8**

**Expansion of lymphotoxin expressing B cells and FRCs proliferation is reduced in mice treated with Sandy-2 (Anti m-BAFF mAb)**

**(a)** FACS profile of inguinal lymph node (iLN) B and T cells after isotype or Sandy-2 mAb treatment. B cells were identified as $CD4^{-}CD8^{-}CD19^{+}MHCII^{+}$. Sandy-2 treatment significantly reduces the B cell numbers in iLN. **(b)** Mice were treated with two doses of isotype control or anti-BAFF (Sandy-2) mAb and infected with *Hp*. mLN gross morphology visualized at 12dpi. **(c)** Representative dot plots showing gating strategy for identification of LTαb-$Fc^{+}$ B cells after isotype or Sandy-2 treatment. **(d)** Representative contour plots showing gating strategy for identification of proliferating FRCs (CD31-MadCAM1-GP38+Ki67+) and LECs after isotype or Sandy-2 treatment. **(e)** Absolute number of proliferating FRCs in mice (treated with isotype or Sandy-2 mAb) post *Hp* infection. Data represent mean ± SEM and representative of two independent experiments with n=3-5 mice/group/time-point. Statistical analyses were performed using ANOVA, Bonferroni's multiple comparison test and significance donated as *$p < 0.05$, **$p < 0.01$, ***$p < 0.001$, and ****$p < 0.0001$.

**Related to Experimental procedure**

**Supplementary Table-1**

| S.No. | Target | Species | Clone | Conjugate | Catalogue No | Supplier |
|---|---|---|---|---|---|---|
| 1 | | | | | | |
| 2 | B220 | Rat | RA3-6B2 | Pacific Blue | 103227 | Biolegend |
| 3 | CD11c | Armenian Hamster | N418 | APC | 117310 | Biolegend |
| 4 | CD19 | Rat | 6D5 | APC | 115512 | Biolegend |
| 5 | CD19 | Rat | 6D5 | APC/fire-750 | 115513 | Biolegend |
| 6 | CD3 | Rat | 17A2 | Alexa 700 | 100216 | Biolegend |
| 7 | CD31 | Rat | 390 | Pacific blue | 102422 | Biolegend |
| 8 | CD31 | Rat | 390 | PE | 102408 | Biolegend |
| 9 | CD35 | Rat | 7E9 | Alexa 488 | 123408 | Biolegend |
| 10 | CD4 | Rat | RM4-5 | PE | 100512 | Biolegend |
| 11 | CD45 | Rat | 30-F11 | Alexa 488 | 103122 | Biolegend |
| 12 | CD45 | Rat | 30-F11 | PEcy7 | 103114 | Biolegend |
| 13 | CD45 | Rat | 30-F11 | Pacific Blue | 103126 | Biolegend |
| 14 | VEGF-A | Rabbit | | Purified | 103-PA03 | Relia Tech Gmbh |
| 15 | GL7 | Rat | GL7 | Biotin | 13-5902-85 | eBiosciences |
| 16 | IgD | Rat | 11-26c.2a | Alexa 700 | 405730 | Biolegend |
| 17 | Isotype Ctr IgG | Rat | RTK2758 | Alexa 488 | 400525 | Biolegend |
| 18 | Isotype Ctr IgG | Rat | RTK4530 | Alexa 700 | 400628 | Biolegend |
| 19 | Isotype Ctr IgG | Rat | eBRG1 | Biotin | 13-4301 | eBiosciences |
| 20 | Ki-67 | Set | B56/MOPC-21 | PE | 556027 | BD Pharmingen |
| 21 | LTbR-Fc | ----- | recombinant | purified | ----- | Biogen Idec |
| 22 | Lyve-1 | Rat | Lyve-1 | Alexa 488 | FAB2125G | R&D systems |
| 23 | MHC Class II | Rat | M5/114.15.2 | Alexa 700 | 107622 | Biolegend |
| 24 | Podoplanin | Syrian Hamster | 8.1.1 | Alexa 647 | in house | Hybridoma |
| 25 | Podoplanin | Syrian Hamster | eBio8.1.1 | eFluor 660 | 50-5381 | eBiosciences |
| 26 | Streptavidin | ----- | ----- | PE | 405204 | Biolegend |
| 27 | Streptavidin | ----- | ----- | APC | 17-4317-82 | eBiosciences |
| 28 | Ter119 | Rat | Ter119 | Varies | 116231/215 | Biolegend |

**Gating strategy**

| | |
|---|---|
| FRCs | Live cells, Ter119-CD45-CD31-MaDCAM1-GP38+ |
| Proliferating FRCs | Live cells, Ter119-CD45-CD31-MaDCAM1-GP38+Ki-67+ |
| LECs | Live cells, Ter119-CD45-CD31+GP38+ |
| Proliferating LECs | Live cells, Ter119-CD45-CD31+GP38+Ki-67+ |
| Naive B cells | Live cells, CD19+IgD+MHCII+ |
| Antigen Activated B cells | Live cells, CD19+IgD-MHCII+ |
| Ltab-Fc+ B cells | Live cells, CD45+B220+Ltab-Fc+ |

**Related to Experimental procedure**

**Supplementary Table-2**

| S.No. | Target | Species | Clone | Conjugate | Catalogue No | Supplier | Dilution |
|---|---|---|---|---|---|---|---|
| | **Primary Antibodies** | | | | | | |
| 1 | B220 | Rat | RA3-6B2 | Biotin | RM2615 | Life Technologies | 1:200 |
| 2 | B220 | Rat | RA3-6B2 | Purified | 103202 | BioLegend | 1:100 |
| 3 | CD3 | Armenain hamster | 145-2C11 | Purified | 100302 | BioLegend | 1:100 |
| 4 | CD35 | Rat | 8C12 | Purified | 558768 | BD Pharmingen | 1:100 |
| 5 | DAPI | ------ | ------ | Powder | D9542 | Sigma-Aldrich | ----- |
| 6 | ER-TR7 | Rat | ER-TR7 | Purified | T-2109 | BMA Biomedicals | 1:200 |
| 7 | FDCs | Rat | FDC-M1 | Purified | 551320 | BD Pharmingen | 1:200 |
| 8 | CD11c | Armenain hamster | N418 | Purified | 117308 | BioLegend | 1:50 |
| 9 | GL7 | Rat | GL7 | Biotin | 13-5902-85 | eBiosciences | 1:50 |
| 10 | Podoplanin (Pdpn) | Syrian Hamster | 8.1.1 | Purified | ------- | Hybridoma | 1:100 |
| 11 | IgD | Rat | 11-26c | Purified | 1120-01 | Southern Biotech | 1:400 |
| 12 | Laminin | Rabbit | ---- | Purified | L9393 | Sigma-Aldrich | 1:200 |
| 13 | Lyve-1 | Rabbit | APA5 | Purified | 103-PA50 | Relia Tech Gmbh | 1:200 |
| 14 | BAFF | Goat | ---- | Purified | AF2106 | R&D systems | 5-10ug/ml |
| 15 | CD31 | Rat | 390 | Purified | ----- | Histology Core (EPFL) | ----- |
| | **Secondary Antibodies** | | | | | | |
| 1 | Anti Armenian hamster | Goat | Polyclonal | Alexa 594 | 127-585-160 | Jackson Immuno Research | 1:400 |
| 2 | Anti Armenian hamster | Goat | Polyclonal | Dylight 594 | 405504 | Biolegend | 1:200 |
| 3 | Anti Rabbit IgG | Donkey | Polyclonal | Alexa 488 | A21206 | Molecular Probes | 1:600 |
| 4 | Anti Rabbit IgG | Donkey | Polyclonal | Alexa 568 | A10042 | Molecular Probes | 1:800 |
| 5 | Anti Rabbit IgG | Donkey | Polyclonal | Alexa 647 | A31573 | Invitrogen | 1:400 |
| 6 | Anti Rat IgG | Donkey | Polyclonal | Alexa 488 | A21208 | Molecular Probes | 1:400 |
| 7 | Anti Rat IgG | Goat | Polyclonal | Alexa 568 | A11077 | Molecular Probes | 1:800 |
| 8 | Anti Rat IgG | Donkey | Polyclonal | Biotin | 712-065-153 | Jackson Immuno Research | 1:200 |
| 9 | Anti Syrian hamster IgG | Goat | Polyclonal | Alexa 647 | 107-606-142 | Jackson Immuno Research | 1:400 |
| 10 | Anti Syrian hamster IgG | Goat | Polyclonal | Alexa 488 | 107-545-142 | Jackson Immuno Research | 1:333 |
| 11 | Streptavidin | ----- | ----- | Alexa 488 | S-11223 | Molecular Probes | 1:800 |
| 12 | Streptavidin | ----- | ----- | Alexa 568 | S-11226 | Molecular Probes | 1:800 |
| 13 | Streptavidin | ----- | ----- | Pacific blue | S-11222 | Invitrogen | 1:100 |
| 14 | Streptavidin | ----- | ----- | Alexa 647 | S-21374 | Invitrogen | 1:800 |